Published in final edited form as:

Mol Cancer Ther. 2014 July ; 13(7): 1690–1703. doi:10.1158/1535-7163.MCT-13-0868.

Leelamine mediates cancer cell death through inhibition of intracellular cholesterol transport

Omer F. Kuzu[1,5], **Raghavendra Gowda**[1,5], **Arati Sharma**[1,5,6], and **Gavin P. Robertson**[1,2,3,4,5,6,7]

[1]Department of Pharmacology, The Pennsylvania State University College of Medicine, Hershey, PA 17033

[2]Department of Pathology, The Pennsylvania State University College of Medicine, Hershey, PA 17033

[3]Department of Dermatology, The Pennsylvania State University College of Medicine, Hershey, PA 17033

[4]Department of Surgery, The Pennsylvania State University College of Medicine, Hershey, PA 17033

[5]Penn State Hershey Melanoma Center, The Pennsylvania State University College of Medicine, Hershey, PA 17033

[6]Penn State Melanoma Therapeutics Program, The Pennsylvania State University College of Medicine, Hershey, PA 17033

[7]The Foreman Foundation for Melanoma Research, The Pennsylvania State University College of Medicine, Hershey, PA 17033

Abstract

Leelamine is a promising compound for the treatment of cancer; however, the molecular mechanisms leading to leelamine-mediated cell death have not been identified. This report shows that leelamine is a weakly basic amine with lysosomotropic properties, leading to its accumulation inside acidic organelles such as lysosomes. This accumulation leads to homeostatic imbalance in the lysosomal endosomal cell compartments that disrupts autophagic flux and intracellular cholesterol trafficking as well as receptor-mediated endocytosis. Electron micrographs of leelamine-treated cancer cells displayed accumulation of autophagosomes, membrane whorls, and lipofuscin-like structures, indicating disruption of lysosomal cell compartments. Early in the process, leelamine-mediated killing was a caspase-independent event triggered by cholesterol accumulation, as depletion of cholesterol using β-cyclodextrin treatment attenuated the cell death and restored the subcellular structures identified by electron microscopy. Protein microarray–based analyses of the intracellular signaling cascades showed alterations in RTK–AKT/STAT/MAPK signaling cascades, which was subsequently confirmed by Western blotting. Inhibition of

Corresponding Author: Gavin P. Robertson, Department of Pharmacology, The Pennsylvania State University College of Medicine, 500 University Drive, Hershey, PA 17033. Phone: (717) 531-8098; Fax: (717) 531-5013; gprobertson@psu.edu.

Conflict of Interest: Penn State has patent protected this discovery, which has subsequently licensed to Melanovus Oncology. Melanovus Oncology is partly owned by Penn State University and Gavin P. Robertson.

Akt, Erk, and Stat signaling, together with abnormal deregulation of receptor tyrosine kinases, was caused by the inhibition of receptor-mediated endocytosis. This study is the first report demonstrating that leelamine is a lysosomotropic, intracellular cholesterol transport inhibitor with potential chemotherapeutic properties leading to inhibition of autophagic flux and induction of cholesterol accumulation in lysosomal/endosomal cell compartments. Importantly, the findings of this study show the potential of leelamine to disrupt cholesterol homeostasis for treatment of advanced-stage cancers.

Keywords

Leelamine; melanoma; lysosomotropism; cholesterol transport inhibitors; autophagy; endocytosis

INTRODUCTION

Melanoma is the deadliest and most metastatic form of skin cancer (1). If it is detected early, surgery still is the most feasible option to cure the disease. However, if it metastasizes to other organs, less than 36% of the patients survive for longer than 1 year (1). Targeted therapies such as Zelboraf and dabrafenib, two U.S. Food and Drug Administration (FDA)–approved mutant B-RAF inhibitors, can be used for the short-term management of melanoma. However, an aggressive drug-resistant disease usually develops, limiting survival benefit to only a few months (2). Cancer cells were able to bypass these targeted therapies by compensating with alternative activation of the mitogen-activated protein kinase (MAPK) pathway, several by activating upstream receptor tyrosine kinases (RTK; ref. 3). Therefore, targeting these alternative escape routes through a combinatorial drug treatment approach or development of a drug that suppresses multiple disease-driving pathways is indispensable for a successful treatment of melanoma or prevention of recurrent resistant disease.

Natural compounds are important sources of new drug development and represent a significant portion of the FDA-approved cancer therapeutics portfolio (4). Through a natural compound library screen, leelamine, a tricyclic diterpene molecule that was extracted from the bark of pine trees, is identified and reported in the article by Gowda and colleagues (in the current issue of this journal) as a potential drug effective against advanced-stage melanoma. This agent has been shown to induce death of advanced-stage melanoma cell lines 3- to 5-fold more effectively than normal cells and has led to a 60% decrease in tumor burden compared with control vehicle-treated animals. In these studies, leelamine inhibited AKT and STAT3 signaling in xenografted tumors. No obvious systemic toxicity of the compound was detected as assessed by body weights of animals or by examination of the various blood parameters that are indicative of organ distress. However, the molecular mechanisms underlying the therapeutic efficacy of leelamine were unknown; therefore, in this report, the mechanism of action of leelamine for induction of cell death in cancer cells has been identified.

Before this study, leelamine was reported to be a poor agonist of cannabinoid receptors (CBR) and a weak inhibitor of pyruvate dehydrogenase kinases (PDK; 5, 6). However, data

presented here suggest that leelamine-mediated melanoma cell death does not involve modulation of any of these reported targets, but was rather initiated by the lysosomotropic property of the compound, which triggers accumulation of compound inside the acidic cell compartments. This accumulation led to the disruption of cholesterol homeostasis and intracellular vesicle transport systems as well as inhibition of autophagic flux. As a consequence, caspase-independent cell death that was separate from classical apoptotic pathways was induced. Western blot analyses revealed inhibition of RTK, AKT, ERK, and STAT3 signaling cascades, which are reported to be important for the survival of melanoma cells. Leelamine-mediated inhibition of these cascades was attributed to the inhibition of receptor-mediated endocytosis of RTKs causing aberrant accumulation of these proteins in the perinuclear region of cells.

MATERIALS AND METHODS

Cell lines, culture conditions and plasmids

Metastatic melanoma cell line UACC 903 was provided by Dr. Mark Nelson (University of Arizona, Tucson, AZ) between 1995 and 1999, 1205 Lu cell line was provided by Dr. Herlyn (Wistar Institute, Philadelphia, PA) between 2003 and 2005, human fibroblast cell line FF2441 was provided by Dr. Craig Myers (Penn State College of Medicine, Hershey, PA) in 2005, and these cell lines were maintained in a cell culture up to 69th, 98th, and 7th passages, respectively. Wild-type and *BAX* knockout (HCT116$BAX^{-/-}$) HCT116 human colon cancer cell lines were provided by Dr. Wafik El-Deiry (Penn State College of Medicine, Hershey, PA) in 2013. Wild-type and *ATG5* knockout (MEF$^{ATG5-/-}$) mouse embryonic fibroblast (MEF) cell lines were provided by Dr. Hong-Gang Wang (Penn State College of Medicine, Hershey, PA) in 2008. All cell lines were maintained in Dulbecco's Modified Eagle Medium (DMEM; Invitrogen) supplemented with 1% GlutaMAX (Invitrogen) and 10% FBS (Hyclone) in a 37°C humidified 5% CO_2 atmosphere incubator. Melanoma cell lines were periodically monitored for genotypic characteristics, phenotypic behavior, and tumorigenic potential to confirm cell line identity. pBABE-puro mCherry-EGFP-LC3B plasmid was obtained from Addgene and transfected to UACC 903 cells to generate GFP-tagged LC3B-expressing UACC 903 cell line (plasmid #22418; ref. 7).

Cell viability assay and drug treatments

Viability of cells upon treatment with various compounds (**see Supplementary Table S1 for compound sources**) was measured through the MTS assay (Promega) as described previously (8). For combinatorial drug treatment studies, both investigated compounds and leelamine were treated simultaneously. However, in the case of β-cyclodextrin pretreatment, β-cyclodextrin was washed away after 60 minutes of treatment and subsequently the cells were treated either with dimethyl sulfoxide (DMSO) or leelamine. Twenty-four hours after treatment, MTS assay was performed.

Caspase dependence, mitochondrial membrane potential and DNA fragmentation assays

Caspase dependence of cell death was measured by growing cells in a 96-well plate and preincubating with pan-caspase inhibitor z-VAD-fmk (20 μmol/L) for 1 hour before drug treatments. TRAIL (50 ng/mL) treatment was used as a positive control for induction of

caspase-dependent cell death. Twenty-four hours after treatment, cell viability was measured by MTS assay. Mitochondrial membrane potential ($\Delta\Psi m$) was measured via the TMRE Mitochondrial Membrane Potential Assay Kit (Abcam) according to the manufacturer's protocol. For the DNA fragmentation assay, total DNA was collected using the DNeasy (Qiagen) Kit according to the instructions and was loaded into 1% agarose gels for electrophoresis.

Electron microscopy analyses

UACC 903 cells growing at 70% to 80% confluency on 35-mm Permanox Petri dishes (Electron Microscopy Sciences) were treated with leelamine (3 μmol/L) alone or incombination with B-cyclodextrin (1 mmol/L) for 3 hours, washed with PBS, and then fixed with fixative (0.5% glutaraldehyde/4% paraformaldehyde in 0.1 mol/L sodium cacodylate buffer, pH 7.3) for 1 hour. The cells were washed in 0.1 mol/L sodium cacodylate and post-fixed overnight in buffered 1% osmium tetroxide and 1.5% potassium ferrocyanide. After post-fixation, cells were rinsed with buffer, dehydrated in a graded series of ethanol, and embedded in EMbed812 (Electron Microscopy Sciences). After sectioning, samples were stained with 2% aqueous uranyl acetate and lead citrate followed by analysis with JEOL JEM1400 Digital Capture transmission electron microscope (TEM).

Kinexus and Receptor Tyrosine Kinase Protein Arrays

UACC 903 cells treated with leelamine (3 μmol/L for 3, 6, 12, or 24 hours) were collected with Kinexus lysis buffer according to the Kinexus protocol and shipped to Kinexus for analyses with Kinexus Antibody Microarray Chip 1.3 (812 antibodies). The array data were normalized through Z-score transformation, and Z-ratios between treated samples and corresponding controls were calculated as described elsewhere (9). The data were analyzed through Ingenuity Pathway Analyses (IPA; version 17199142) software based on the alterations with a Z-ratio > 1.5 or Z-ratio < −1.5 with the software's default settings. The Human Phospho-Receptor Tyrosine Kinase Array Kit was obtained from R&D Systems, and experiments were performed according to the manufacturer's protocols. The blot images were quantified using Quantity One 1-D Software (Bio-Rad Laboratories).

Cholesterol localization, quantitation and TLC analyses

Localization of intracellular cholesterol was detected through Cayman's Cholesterol Cell-Based Detection Assay Kit (Cayman Chemical) according to the manufacturer's protocol. Lipid extraction from cell cultures was achieved through the Bligh and Dyer method (10). The lipid extract was dissolved in chloroform:methanol (2:1) and stored at −20°C. Thin layer chromatography (TLC) analyses were undertaken according to a published approach (11). High-performance TLC (HPTLC) Silica gel 60 plates (Merck) were developed with iodine vapor. The bands were analyzed with ImageJ, an image analysis software (v1.44; NIH, Bethesda, MD). Retention factors were calculated as 0.35 for cholesterol, 0.1 for phosphatidylcholine, and 0.17 for phosphatidylethanolamine. These values were consistent with the values observed in the aforementioned published study (11).

Evaluation of endocytosis

Endocytic capacity of the cells was measured through evaluation of receptor-mediated endocytosis of Alexa Fluor 488–conjugated transferrin protein (Molecular Probes). Briefly, cells were seeded into chamber slides and treated with leelamine for 2 hours. Next, transferrin protein was added at a final concentration of 5 μg/mL and incubated for 30 minutes. Cells were then washed with PBS, trypsinized, and collected for flow cytometry analysis or fixed on a slide with 4% paraformaldehyde for fluorescence microscopy analysis.

Analyses of drug uptake using ^{3}H-labeled leelamine

To analyze the kinetics of leelamine uptake, 3H-labeled leelamine was used (specific activity of 25 Ci/mmol; American Radio Chemicals Inc.). UACC 903 cells (70%–85% confluent in a 150-mm plate) were treated with 25 mL of DMEM containing 3 μmol/L leelamine and 5 μL of 20 μmol/L triated leelamine (1 million CPM/μL). At various time points, 20 μL of media from the plate was collected and radioactivity associated with the tritiated leelamine was measured using the LS-6500-Beckman Coulter liquid scintillation counter.

Analyses of lysosomotropism

UACC 903 cells were plated into 6-well plate and grown to 75% to 90% confluency. Cells were treated with 1 μmol/L LysoTracker Red DND-99 (Life Technologies) for 15 minutes. Cells were subsequently treated with leelamine or chloroquine for 45 minutes and collected for flow cytometry analysis.

Western blot analysis

Melanoma cells (1–1.5 × 106) were plated in 100-mm culture dishes and grown to 75% to 90% confluency. After treatments, at indicated time points, cells were harvested in radioimmunoprecipitation assay (RIPA) buffer containing protease and phosphatase inhibitors (Pierce Biotechnology). Proteins were quantitated using the BCA assay from Pierce. Thirty micrograms of protein per lane was loaded onto a NuPage gel from Life Technologies and electrophoresed according to the manufacturer's instructions. Proteins were transferred to polyvinylidene difluoride (PVDF) membrane, and blots were probed with antibodies according to the supplier's recommendations (for detailed antibody information, see Supplementary Table S2). Immunoblots were developed using the enhanced chemiluminescence (ECL) detection system (Thermo Fisher Scientific).

siRNA transfections

siRNA (1 pmol/well) was transfected into UACC 903 cells that were seeded into 96-well plates using Lipofectamine RNAiMAX (Life Technologies) reagent according to the manufacturer's protocols. Forty-eight hours after transfection, effect on cell viability was measured by MTS assays. Mutant BRAF siRNA and scrambled siRNA were used as positive and negative controls, respectively. Viability of cells was plotted against scrambled siRNA-transfected cells (siRNA sequences are provided in Supplementary Table S3).

Statistical Analysis

The statistical analysis was performed using the unpaired Student t test. A $P < 0.05$ was considered statistically significant. * indicates $P < 0.05$.

RESULTS

Leelamine inhibits autophagic flux in melanoma cells

To dissect the mechanism by which leelamine kills cancer cells, UACC 903 melanoma cells treated with leelamine were examined by light and electron microscopy. Light microscopy showed rapid and widespread vacuolization of the cells (Fig. 1A), followed by membrane blebbing, cell shrinkage, and cell rounding. Compared with control DMSO-treated cells (Fig. 1B, box a), TEM showed accumulation of lipofuscin-like material (Fig. 1B, box b; undegraded lysosomal waste), formation of web-like membrane whorls (Fig. 1B, box c), and increased number of autophagosomes (Fig. 1B, box d).

TEM analysis suggested that leelamine treatment led to autophagosome accumulation; therefore, the effect of leelamine on autophagic flux was next evaluated through Western blotting. Treatment with Bafilomycin A1 (BafA1), a specific inhibitor of vacuolar type H+-ATPase that blocks autophagic flux, induced accumulation of LC3B (an autophagosome marker) and p62/SQSTM1 (an autophagic flux marker) proteins, indicating the inhibition of autophagosome degradation (Fig. 1C; ref. 12). Likewise, leelamine treatment induced the accumulation of both proteins in a dose-dependent manner, suggesting inhibition of autophagic flux. Accumulation of LC3B protein was detectable via fluorescence microscopy of UACC 903 cells expressing GFP-tagged LC3B protein (Fig. 1C). Leelamine treatment also dose-dependently increased the intensity ratio of LC3B-II to LC3B-I, further indicating enhanced autophagic activity (Fig. 1C).

Leelamine possesses lysosomotropic property leading to accumulation inside the acidic cell compartments

Because observations such as vacuolization of cells, accumulation of lipofuscin-like material, formation of web-like membrane whorls, and inhibition of autophagic flux are commonly attributed to lysosomal storage diseases and can be mimicked by some lysosomotropic compounds, the lysosomotropic potential of leelamine was next investigated (13, 14). As a weakly basic primary amine, leelamine has a pKa of 9.9 (calculated by ACD Labs Precepta software v14.0), and it was therefore predicted to be a lysosomotropic compound. Treatment with vacuolar H+-ATPase inhibitors can suppress the activity of lysosomotropic compounds by inhibiting the acidification of cell compartments (15). Pretreatment of UACC 903 melanoma cells with two vacuolar H+-ATPase inhibitors that target different subunits of the H+-ATPase complex, BafA1 and Concanamycin A (Conc-A), suppressed leelamine-mediated cell vacuolization (Fig. 1D), suggesting that leelamine is a lysosomotropic compound.

Lysosomotropic compounds can be rapidly taken up by cells due to trapping inside the acidic organelles such as lysosomes and late endosomes (16, 17). To measure the kinetics of leelamine uptake, UACC 903 cells were treated with tritiated leelamine, and every 10

minutes, media samples were collected to quantify levels of tritiated compound remaining in the media. Sixty percent of the tritiated leelamine was internalized into cells in less than 30 minutes after treatment, which supports the lysosomotropic property of the compound (Fig. 1E). This was further confirmed by testing the efficacy of collected samples to decrease cell viability. UACC 903 cells were treated with 3 μmol/L leelamine in a p100 plate, and every 10 minutes, 300 μL of media was collected from the plate to treat UACC 903 cells that were plated in a 96-well plate (100 μL × 3 wells/sample). Twenty-four hours later, cell viability was assessed by MTS assay. Consistent with the uptake kinetics of leelamine, samples collected 30 minutes after preincubation with cells did not induce cell death in UACC 903 cells (Fig. 1F).

To further validate the lysosomotropic property of leelamine, a modified LysoTracker Red DND-99 competition assay was used (18). Lysosomotropic compounds typically compete with LysoTracker Red DND-99 to decrease uptake. Therefore, cells treated with a lysosomotropic compound should take up less LysoTracker Red DND-99. Flow cytometry–based quantitation of the staining of cells with the LysoTracker Red DND-99 showed decreased uptake following treatment with chloroquine (100 μmol/L), a well-known lysosomotropic compound, or leelamine (3 μmol/L), which provided further support for leelamine as a lysosomotropic compound (Fig. 1G).

Lysosomotropic property of leelamine mediated early caspase-independent melanoma cell death

To determine whether the lysosomotropic property of leelamine mediated its activity, cell viability following H+-ATPase inhibition was measured. Cotreatment of 10 nmol/L of BafA1 or Conc-A effectively protected melanoma cells from leelamine-mediated cell death (Fig. 2A). Moreover, abietic acid, a structurally similar compound to leelamine that lacks the amine group, failed to induce either vacuolization or death of UACC 903 cells, suggesting that the amine group of leelamine mediated its lysosomotropic activity to subsequently trigger cell death (Supplementary Fig. S1).

Although leelamine has been reported in the current issue of this journal to induce the activation of caspases (Gowda and colleagues), it was not known whether the fate of leelamine-treated cells is solely a result of caspase activation, or if there are other players that trigger cell death. In the case of caspase-dependent cell death, it would be expected that inhibition of caspase activation via pan-caspase inhibitor zVAD-fmk would rescue cells from leelamine-mediated cell death. In the positive control, zVAD-fmk cotreatment completely restored the viability of cells, which was reduced to 58% by TRAIL treatment (Fig. 2B). In contrast, zVAD-fmk had no effect on the viability of melanoma cells when cotreated with leelamine. Furthermore, leelamine did not induce caspase-mediated DNA fragmentation up to 24 hours following treatment when compared with Staurosporine treatment, an accepted apoptosis inducer (Fig. 2C; ref. 19). This observation indicated that early phase of leelamine-mediated cell death was triggered through a caspase-independent process despite the fact that caspases are activated downstream in the cell death process.

Because various caspase-independent cell death programs require de novo protein synthesis, the effect of inhibition of protein synthesis on leelamine-mediated cell death was examined

next (20). Cotreatment of UACC 903 melanoma cells with cycloheximide, a protein synthesis inhibitor, did not affect viability of leelamine-treated cells, suggesting that de novo protein synthesis is not required for leelamine-mediated cell death (Supplementary Fig. S2A).

Lysosomotropic compounds can induce caspase-independent cell death through lysosomal membrane permeabilization leading to leakage of cathepsins (lysosomal peptidases) into the cytosol (17, 21). To examine whether leelamine caused lysosomal membrane permeabilization, lysosomal peptidase inhibitors, ALLN (calpain/cathepsin-inhibitor 1), ALLM (calpain/cathepsin-inhibitor 2), leupeptin (cysteine, serine, and threonine peptidase inhibitor), Pepstatin-A (aspartic proteinase inhibitor), and AEBSF (irreversible serine protease inhibitor), were used. However, none of these inhibitors were able to alter leelamine-mediated cell death, suggesting that lysosomal membrane permeabilization is not involved in leelamine-mediated cell death (Supplementary Fig. S2B).

Because disruption of mitochondrial function plays a key role in the execution of several cell death programs, mitochondrial membrane potential ($\Delta\Psi m$) of UACC 903 cells was measured after leelamine treatment (22). In the positive control, 20 μmol/L of FCCP, a very potent uncoupler of oxidative phosphorylation, significantly hindered $\Delta\Psi m$ of treated cells. Leelamine treatment also decreased the $\Delta\Psi m$ of treated melanoma cells in a time- and dose-dependent manner (Fig. 2D). Of note, $\Delta\Psi m$ was found to be diminished in more than 70% of the cells when melanoma cells were treated with 3 μmol/L leelamine for 24 hours, suggesting that leelamine triggers significant perturbations in mitochondrial stability.

Bcl-2–associated X protein (BAX) and BH3 interacting-domain death agonist (BID) are two well-studied apoptosis regulators that induce the opening of the mitochondrial voltage-dependent anion channels following apoptotic signals (23). The potential involvement of BAX in leelamine-mediated cell death was investigated through comparing wild-type HCT116 cells with BAX knockout HCT116 (HCT116BAX−/−) cells. Interestingly, BAX knockout cells were more resistant to leelamine-mediated cell death in contrast to their wild-type counterparts (Fig. 2E). However, contradictorily, pharmacologic inhibition of BAX channels through Bax-inhibiting peptide, V5, inhibition of BID activity through BI-6C9, or inhibition of apoptosome formation by NS3694 was not able to suppress leelamine-mediated cell death (Supplementary Fig. S2C).

Blockage of autophagic flux mediated by leelamine

Lysosomotropic compounds can block autophagic flux through alkalinization of the lysosome to trigger caspase-independent cell death (17, 21). To investigate whether leelamine-mediated cell death involves inhibition of autophagic flux, autophagy-deficient ATG5 knockout MEFs cells were compared with wild-type counterparts following leelamine treatment. ATG5 knockout MEFs showed partial resistance to leelamine-mediated cell death, suggesting that inhibition of autophagic flux played an important role in this process (Fig. 2F). Interestingly, ATG5 knockout MEF cells did not undergo vacuolization upon leelamine treatment, indicating a relationship between vacuolization and autophagy (Fig. 2F). Thus, leelamine-mediated cell death was associated with its lysosomotropic property and partially involved inhibition of autophagic flux.

Activity of leelamine was not mediated by PDKs or CBRs

Pyruvate dehydrogenase kinases (PDK) and cannabinoid receptors (CBR) are reported targets of leelamine (5, 6, 24). To determine whether leelamine-mediated cell death involved any of these proteins, pharmacologic agents or RNA interference was used to inhibit these proteins. siRNA-mediated knockdown of PDK isoforms or dichloroacetate-mediated inhibition of PDKs did not affect the viability of melanoma cells, suggesting that PDKs are not mediating the effect (Supplementary Fig. S3A and S3B). Agonists of CBRs have also been reported to promote apoptotic cell death in melanoma cells (25); however, cotreatment of neither CB1 inverse antagonist AM251, nor CB2 inverse antagonist AM630, nor a combination of them, protected UACC 903 cells from leelamine-mediated cell death (Supplementary Fig. S3C). Consistent with these observations, siRNA-mediated knockdown of CBRs also failed to alter the activity of leelamine (Supplementary Fig. S3D). Thus, none of the reported targets of leelamine were found to mediate the chemotherepeutic activity of the compound.

Leelamine induced intracellular cholesterol accumulation and altered cholesterol subcellular localization

Phenotypes induced by some lysosomotropic compounds (e.g., U18666A and imipramine) resemble those occurring with Niemann–Pick type C (NPC) disease (26, 27). NPC is a well-studied lysosomal storage disease, which leads to neurodegeneration and cell death through late endosomal/lysosomal (LE/L) accumulation of unesterified cholesterol due to loss-of-function mutations in NPC proteins (28). These compounds also lead to the accumulation of endosomal cholesterol upon treatment (26, 27). To investigate whether leelamine triggered a phenotype similar to NPC, cholesterol localization following leelamine treatment was analyzed via Filipin-III staining. Under steady-state conditions, UACC 903 cells stained weakly for Filipin at the periphery of the nucleus (Fig. 3A). Of note, 3 μmol/L leelamine significantly altered cholesterol localization and induced a staining pattern, which was comparable with that occurring following U18666A treatment (Fig. 3A). At higher concentrations (5 μmol/L), cholesterol accumulation was more significant and observed as large droplets around the nucleus. In contrast, altered cholesterol localization was not observed in normal fibroblasts at the 3 μmol/L, but was significant at 10 μmol/L. β-cyclodextrin–mediated depletion of cholesterol has been reported to decrease the toxicity of cholesterol accumulation in NPC disease (29). Cotreatment of β-cyclodextrin prevented intracellular cholesterol accumulation even at high leelamine concentrations (Fig. 3A). TLC analyses of the lipid extracts from UACC 903 cells showed an increase in intracellular cholesterol accumulation following leelamine treatment (Fig. 3B).

To validate the biologic significance of leelamine-mediated cholesterol accumulation, β-cyclodextrin was used to deplete cellular cholesterol levels. Depletion of cholesterol from UACC 903 or 1205 Lu melanoma cells through pre- or cotreatment with β-cyclodextrin suppressed cell death mediated by leelamine treatment (Fig. 3C). In addition, electron microscopy analysis of the β-cyclodextrin–cotreated UACC 903 cells showed that depletion of cholesterol prevented formation of lipofuscin-like material, membrane whorls, and autophagic vesicles observed following leelamine treatment (Fig. 3D). It is important to note

that the inhibition of cholesterol transport but not the cholesterol synthesis led to cell death, as statins were not able to induce cell death in these cell lines (Supplementary Fig. S4).

Leelamine inhibited cellular endocytosis

Endosomes are major sorting compartments within cells functioning not only for the uptake of extracellular material, but also for the maintenance of cell signaling through recycling of membrane receptors (30, 31). Because endosomal accumulation of cholesterol has the potential to disrupt the endocytic system, the integrity of the system was assessed by measuring endocytic uptake of Alexa Fluor–conjugated transferrin protein (32, 33). Fluorescence microscopy analysis showed robust suppression of endocytosis following leelamine treatment for both UACC 903 and 1205 Lu melanoma cells (Fig. 3E). Depletion of cholesterol through β-cyclodextrin cotreatment prevented leelamine-mediated inhibition of transferrin endocytosis. In contrast, although endocytosis of transferrin was restricted in fibroblasts cells, its inhibition was not seen until the leelamine concentration was increased to 10 μmol/L (Fig. 3E). Flow cytometry–based quantitation of transferrin signal confirmed the fluorescence microscopy analysis and displayed a dose-dependent inhibition of endocytosis (Fig. 3F). Of note, 3 μmol/L leelamine treatment decreased endocytosis-positive UACC 903 cells by 68% while 5 μmol/L decreased it by 88%. Collectively, these data suggest that leelamine treatment inhibited cellular endocytosis in cancer cells at 3 μmol/L and required 3-fold higher levels to see a similar effect in normal cells.

Leelamine inhibited signaling pathways driving melanoma cell survival

Because leelamine disrupted cellular endocytosis, inhibition of this process was predicted to disrupt key signaling pathways important for melanoma survival. Therefore, signaling pathways altered following leelamine treatment were assessed. Since cycloheximide treatment suggested that protein synthesis was not involved in the activity of leelamine, the primary effect of the compound was predicted to occur at the posttranslational level. Therefore, to assess these changes, high-throughput antibody microarray analysis was undertaken using Kinexus Antibody Microarray Chip 1.3 (Kinexus Bioinformatics Corporation). This analysis simultaneously assessed the expression and phosphorylation status of various cell signaling proteins. Cell lysates were collected at various time points from 3 to 24 hours following leelamine or control treatment and analyzed using the Kinexus arrays. Data were normalized through Z-score transformation and significant alterations were identified by calculation of Z-ratios between treated samples and corresponding controls (Table 1; see Supplementary Table S4 for array results). Results suggested alterations in the members of the RTK–AKT signaling pathway [e.g., insulin—like growth factor 1 receptor (IGF1R), IRS1, ALK, EPHA1, ERBB2, GSK3, and FOXO3 (FKHRL1); Fig. 4A]. Analyzes of the data through IPA software suggested that the insulin and phosphoinositide 3-kinase (PI3K)–AKT pathways were the most prominent pathways that were altered following leelamine treatment (Supplementary Fig. S5).

Involvement of key proteins that were downstream of RTK signaling was subsequently validated by Western blotting. Significant suppression of the active AKT (pAKT) and STAT3 proteins (pSTAT3) was identified (Fig. 4B). Suppression of several other signaling proteins [e.g., MAPK3/MAPK1 (Erk1/2), AKT1S1 (PRAS40), CREB, and RPS6KB1

(p70S6K)] in these pathways has been validated by Gowda and colleagues in the current issue of this journal. Phosphorylation of EIF4EBP1 (4E-BP1), an important regulator of cap-dependent protein translation, was significantly decreased by leelamine, suggesting that the AKT/mTOR branch of the cascade was also inhibited following leelamine treatment (34). Most importantly, BafA1 cotreatment reversed the effect of leelamine on these signaling cascades, suggesting that these alterations were triggered by the lysosomotropic properties of leelamine (Fig. 4B).

Leelamine disrupted RTK signaling via interference with intracellular vesicular transport systems, which was reversible by cholesterol depletion

Because protein microarray analysis suggested alterations in RTK signaling, the activities of 42 different RTKs were analyzed using a protein array that is specific to RTKs (Fig. 4C). Alterations in tyrosine phosphorylation of several RTKs, such as decreases in ERBB4 and platelet—derived growth factor receptor (PDGFR) receptors, as well as an increase in IGF1R and hepatocyte growth factor receptor (HGFR) receptors were observed. However, identified increases in HGFR and IGF1R phosphorylation were associated with intracellular accumulation of these receptors. Western blot analyses displayed a dose- and time-dependent accumulation of HGFR precursor protein with significant decrease in mature forms of both HGFR and IGF1R receptors (Fig. 4D). The precursor form of IGF1R also displayed slight accumulation that was more significant after 12 hours of leelamine treatment. Accumulation of these precursor proteins were possibly related to the disruption of the endocytic system (35). Moreover, immunofluorescence staining of various RTKs (IGF1R, PDGFR, and TRK receptors) and IRS1, an adaptor protein in INSR/IGF1R-AKT signaling, displayed perinuclear accumulation, further supporting inhibition of the intracellular vesicular transport system (Fig. 4E).

To demonstrate that signaling alterations were induced by disrupted cholesterol homeostasis, β-cyclodextrin cotreatment was used to deplete cholesterol, and effects on inhibited signaling pathways were examined by Western blotting (Fig. 4F). β-cyclodextrin cotreatment restored phosphorylation of AKT and STAT3 proteins, suppressed accumulation of IGF1R and HGFR precursors, inhibited upregulation of CDKN1B (p27) protein, reinstated CCND1 (cyclin D1) to control levels, and decreased PARP cleavage (Fig. 4F). Thus, these observations suggested that leelamine-mediated signaling alterations were initiated by disruption of cholesterol homeostasis leading to shutdown of cellular endocytosis.

DISCUSSION

In this study, leelamine has been identified as a lysosomotropic compound that disrupts intracellular cholesterol homeostasis to induce cell death more selectively in melanoma cells compared to normal cells. Cholesterol is an essential component of cell membranes and occupies vital roles in intracellular transport and signaling systems (36, 37). Its homeostasis is strictly regulated as proper functioning of several organelles, such as golgi, endoplasmic reticulum, and mitochondria, relies on cholesterol abundance in the membranes of these organelles (38, 39). Late endosomes and lysosomes have an important role in maintaining

this homeostasis. Cholesterol that is derived from the membranes of the endocytotic vesicles and cholesteryl esters that are derived from the imported low-density lipoprotein (LDL) molecules or from the autophagic flux, converge on the lysosomal cell compartments where cholesteryl esters are hydrolyzed to free cholesterol molecules (39–41). Excess free cholesterol should be either esterified in the endoplasmic reticulum or removed from the cell through the efflux pathway (39). NPC1 and NPC2 proteins function together to export free cholesterol from the LE/L cell compartments, and loss-of-function mutations in these genes give rise to the accumulation of free cholesterol in the LE/L compartments (42). Because lysosomes are a convergent point for the endocytic and autophagic pathways, cholesterol accumulation potentially shuts down both of these pathways.

Inhibition of autophagic flux is potentially detrimental to cells due to insufficient disposal of toxic protein aggregates and inadequate recycling of unnecessary cellular components to maintain intracellular homeostasis (17). Recent studies link autophagy to cholesterol homeostasis (41). Elrick and colleagues identified autophagy as an important source of accumulated cholesterol in NPC disease (43). In their study, ATG5-null-MEF cells accumulated less cholesterol in the LE/L compartments upon U18666A treatment. In agreement with this observation, ATG5-null-MEF cells were more resistant to leelamine-mediated cell death compared with wild-type counterparts. These observations suggested autophagy as an important source for accumulated cholesterol in leelamine-treated cells. Moreover, endosomal cholesterol accumulation not only inhibits autophagic flux but can also induce autophagy itself (44). Leelamine treatment dose-dependently increased LC3BII to LC3BI ratio, as well as decreased the phosphorylation of 4EBP1, suggesting the sustained inhibition of mTOR signaling and induction of autophagy. Thus, the autophagic process creates a vicious cycle between cholesterol accumulation and autophagy induction in which endosomal cholesterol accumulation triggers autophagy, and autophagy subsequently induces further endosomal cholesterol accumulation, which is summarized in Fig. 5.

In contrast to autophagy, inhibition of endocytosis disrupts intracellular signaling processes, as receptor mediated signaling depends on endocytosis and endocytic recycling of internalized receptors to the cell membrane (45). RTKs are an important family of membrane receptors that are regulated through receptor-mediated endocytosis. Upon ligand binding and activation, they are internalized through endocytosis and transported to the late endosomes where they are either recycled back to the membrane or directed to the lysosomes for degradation (45). This process is important for downregulation of initiated signal transduction and also is required for transduction of various signals from the cell periphery to the nucleus (46).

RTKs play vital roles in the progression of several cancers including melanoma (47). Hyperactivation of several RTKs, such as PDGFR, ERBB4, AXL, and IGF1R, contribute to mutant BRAF inhibitor resistance (3). They induce PI3K–AKT, Stat, and mitogen—activated protein kinase (MAPK) signaling cascades in response to extracellular factors. Leelamine-mediated disruption of RTK signaling led to the inhibition of these three signaling cascades. However, inhibition of MAPK signaling was not very prominent in contrast to AKT3 and STAT3 pathway shutdown, as the constitutive activation of the MAPK cascade is triggered by mutant V600EBRAF protein and does not require RTK

activity (48). Silencing of AKT activity significantly suppresses melanoma tumor growth (49). Cell lines with over-activated AKT signaling show increased sensitivity to the inhibition of the PI3K–AKT signaling pathway (50). Because leelamine inhibits Akt signaling, it is effective for killing cells in which the PI3K pathway is activated. RTKs also mediate induction of Stat signaling, which is reported to be essential for the transforming activity of the various RTKs such as IGF1R (51). Under steady-state growth conditions, activity of STAT proteins is transient and tightly regulated by various signaling pathways (52). However, STATs are constitutively activated and promote tumor development in several malignancies, including melanoma (53). Niu and colleagues reported constitutive activation of STAT3 in more than 80% of melanoma cell lines in which hyperactivated STAT3 inhibits apoptotic pathways through induction of BCL2L1 (BCL-XL) expression (54). Our studies showed that leelamine significantly hinders STAT3 activity and decreases BCL2L1 protein levels as observed in Kinexus array analysis and in subsequent validation studies.

In summary, this study identifies leelamine as a lysosomotropic agent that triggers cell death through cholesterol accumulation in LE/L cell compartments. The accumulated cholesterol inhibits autophagic flux, disrupts receptor-mediated endocytosis, and subsequently inhibits signaling pathways that are key to melanoma development. These findings not only suggest significant potential of leelamine for the treatment of melanoma, but also identify a new approach for induction of melanoma cell death and possibly that of other cancer types.

Supplementary Material

Refer to Web version on PubMed Central for supplementary material.

ACKNOWLEDGEMENTS

The authors thank Drs. Wolfgang Muss, Patrice Petit, Ken Hastings, Goodwin Jinesh, and Jayanta Debnath for their guidance in interpretation of the electronmicrographs.

Grant Support: NIH grants R01 CA-136667-02, RO1 CA-1138634-02, RO1 CA-127892-01A (G. P. Robertson), The Foreman Foundation for Melanoma Research (G. P. Robertson) and H.G. Barsumian, M.D. Memorial Fund (A. Sharma).

REFERENCES

1. Tas F. Metastatic behavior in melanoma: timing, pattern, survival, and influencing factors. J Oncol. 2012; 2012:647684. [PubMed: 22792102]
2. Wang AX, Qi XY. Targeting RAS/RAF/MEK/ERK signaling in metastatic melanoma. IUBMB Life. 2013; 65:748–758. [PubMed: 23893853]
3. Finn L, Markovic SN, Joseph RW. Therapy for metastatic melanoma: the past, present, and future. BMC Med. 2012; 10:23. [PubMed: 22385436]
4. Newman DJ, Cragg GM. Natural products as sources of new drugs over the last 25 years. J Nat Prod. 2007; 70:461–477. [PubMed: 17309302]
5. Aicher TD, Damon RE, Koletar J, Vinluan CC, Brand LJ, Gao J, et al. Triterpene and diterpene inhibitors of pyruvate dehydrogenase kinase (PDK). Bioorg Med Chem Lett. 1999; 9:2223–2238. [PubMed: 10465550]
6. Lovinger DM. Presynaptic modulation by endocannabinoids. Handb Exp Pharmacol. 2008:435–477. [PubMed: 18064422]

7. N'Diaye EN, Kajihara KK, Hsieh I, Morisaki H, Debnath J, Brown EJ. PLIC proteins or ubiquilins regulate autophagy-dependent cell survival during nutrient starvation. EMBO Rep. 2009; 10:173–179. [PubMed: 19148225]
8. Gowda R, Madhunapantula SV, Desai D, Amin S, Robertson GP. Selenium-containing histone deacetylase inhibitors for melanoma management. Cancer Biol Ther. 2012; 13:756–765. [PubMed: 22669577]
9. Cheadle C, Vawter MP, Freed WJ, Becker KG. Analysis of microarray data using Z score transformation. J Mol Diagn. 2003; 5:73–81. [PubMed: 12707371]
10. Bligh EG, Dyer WJ. A rapid method of total lipid extraction and purification. Can J Biochem Physiol. 1959; 37:911–917. [PubMed: 13671378]
11. Kupke IR, Zeugner S. Quantitative high-performance thin-layer chromatography of lipids in plasma and liver homogenates after direct application of 0.5-microliter samples to the silica-gel layer. J Chromatogr. 1978; 146:261–271. [PubMed: 212444]
12. Klionsky DJ, Abeliovich H, Agostinis P, Agrawal DK, Aliev G, Askew DS, et al. Guidelines for the use and interpretation of assays for monitoring autophagy in higher eukaryotes. Autophagy. 2008; 4:151–175. [PubMed: 18188003]
13. Settembre C, Fraldi A, Jahreiss L, Spampanato C, Venturi C, Medina D, et al. A block of autophagy in lysosomal storage disorders. Hum Mol Genet. 2008; 17:119–129. [PubMed: 17913701]
14. Futerman AH, van Meer G. The cell biology of lysosomal storage disorders. Nat Rev Mol Cell Biol. 2004; 5:554–565. [PubMed: 15232573]
15. Marceau F, Bawolak MT, Lodge R, Bouthillier J, Gagne-Henley A, Gaudreault RC, et al. Cation trapping by cellular acidic compartments: beyond the concept of lysosomotropic drugs. Toxicol Appl Pharmacol. 2012; 259:1–12. [PubMed: 22198553]
16. Ishizaki J, Yokogawa K, Ichimura F, Ohkuma S. Uptake of imipramine in rat liver lysosomes in vitro and its inhibition by basic drugs. J Pharmacol Exp Ther. 2000; 294:1088–1098. [PubMed: 10945864]
17. Geng Y, Kohli L, Klocke BJ, Roth KA. Chloroquine-induced autophagic vacuole accumulation and cell death in glioma cells is p53 independent. Neuro Oncol. 2010; 12:473–481. [PubMed: 20406898]
18. Lemieux B, Percival MD, Falgueyret JP. Quantitation of the lysosomotropic character of cationic amphiphilic drugs using the fluorescent basic amine Red DND-99. Anal Biochem. 2004; 327:247–251. [PubMed: 15051542]
19. Belmokhtar CA, Hillion J, Segal-Bendirdjian E. Staurosporine induces apoptosis through both caspase-dependent and caspase-independent mechanisms. Oncogene. 2001; 20:3354–3362. [PubMed: 11423986]
20. Liu CY, Takemasa A, Liles WC, Goodman RB, Jonas M, Rosen H, et al. Broad-spectrum caspase inhibition paradoxically augments cell death in TNF-alpha -stimulated neutrophils. Blood. 2003; 101:295–304. [PubMed: 12393619]
21. Boya P, Kroemer G. Lysosomal membrane permeabilization in cell death. Oncogene. 2008; 27:6434–6451. [PubMed: 18955971]
22. Chen LB. Mitochondrial membrane potential in living cells. Annu Rev Cell Biol. 1988; 4:155–181. [PubMed: 3058159]
23. Shimizu S, Narita M, Tsujimoto Y. Bcl-2 family proteins regulate the release of apoptogenic cytochrome c by the mitochondrial channel VDAC. Nature. 1999; 399:483–487. [PubMed: 10365962]
24. Cadoudal T, Distel E, Durant S, Fouque F, Blouin JM, Collinet M, et al. Pyruvate dehydrogenase kinase 4: regulation by thiazolidinediones and implication in glyceroneogenesis in adipose tissue. Diabetes. 2008; 57:2272–2279. [PubMed: 18519799]
25. Blazquez C, Carracedo A, Barrado L, Real PJ, Fernandez-Luna JL, Velasco G, et al. Cannabinoid receptors as novel targets for the treatment of melanoma. FASEB J. 2006; 20:2633–2635. [PubMed: 17065222]

26. Kobayashi T, Beuchat MH, Lindsay M, Frias S, Palmiter RD, Sakuraba H, et al. Late endosomal membranes rich in lysobisphosphatidic acid regulate cholesterol transport. Nat Cell Biol. 1999; 1:113–118. [PubMed: 10559883]
27. Lange Y, Ye J, Rigney M, Steck T. Cholesterol movement in Niemann-Pick type C cells and in cells treated with amphiphiles. J Biol Chem. 2000; 275:17468–17475. [PubMed: 10751394]
28. Schneider P, Korolenko TA, Busch U. A review of drug-induced lysosomal disorders of the liver in man and laboratory animals. Microsc Res Tech. 1997; 36:253–275. [PubMed: 9140926]
29. Matsuo M, Togawa M, Hirabaru K, Mochinaga S, Narita A, Adachi M, et al. Effects of cyclodextrin in two patients with Niemann-Pick Type C disease. Mol Genet Metab. 2013; 108:76–81. [PubMed: 23218948]
30. Mellman I. Endocytosis and molecular sorting. Annu Rev Cell Dev Biol. 1996; 12:575–625. [PubMed: 8970738]
31. Maxfield FR, McGraw TE. Endocytic recycling. Nat Rev Mol Cell Biol. 2004; 5:121–132. [PubMed: 15040445]
32. Sobo K, Le Blanc I, Luyet PP, Fivaz M, Ferguson C, Parton RG, et al. Late endosomal cholesterol accumulation leads to impaired intra-endosomal trafficking. PLoS One. 2007; 2:e851. [PubMed: 17786222]
33. Zhang M, Dwyer NK, Love DC, Cooney A, Comly M, Neufeld E, et al. Cessation of rapid late endosomal tubulovesicular trafficking in Niemann-Pick type C1 disease. Proc Natl Acad Sci U S A. 2001; 98:4466–4471. [PubMed: 11296289]
34. Pause A, Belsham GJ, Gingras AC, Donze O, Lin TA, Lawrence JC Jr, et al. Insulin-dependent stimulation of protein synthesis by phosphorylation of a regulator of 5'-cap function. Nature. 1994; 371:762–767. [PubMed: 7935836]
35. Basque J, Martel M, Leduc R, Cantin AM. Lysosomotropic drugs inhibit maturation of transforming growth factor-beta. Can J Physiol Pharmacol. 2008; 86:606–612. [PubMed: 18758509]
36. Incardona JP, Eaton S. Cholesterol in signal transduction. Curr Opin Cell Biol. 2000; 12:193–203. [PubMed: 10712926]
37. Wang Y, Thiele C, Huttner WB. Cholesterol is required for the formation of regulated and constitutive secretory vesicles from the trans-Golgi network. Traffic. 2000; 1:952–962. [PubMed: 11208085]
38. Bastiaanse EM, Hold KM, Van der Laarse A. The effect of membrane cholesterol content on ion transport processes in plasma membranes. Cardiovasc Res. 1997; 33:272–283. [PubMed: 9074689]
39. Simons K, Ikonen E. How cells handle cholesterol. Science. 2000; 290:1721–1726. [PubMed: 11099405]
40. Liscum L, Faust JR. The intracellular transport of low density lipoprotein-derived cholesterol is inhibited in Chinese hamster ovary cells cultured with 3-beta-[2-(diethylamino)ethoxy]androst-5-en-17-one. J Biol Chem. 1989; 264:11796–11806. [PubMed: 2745416]
41. Ouimet M, Franklin V, Mak E, Liao X, Tabas I, Marcel YL. Autophagy regulates cholesterol efflux from macrophage foam cells via lysosomal acid lipase. Cell Metab. 2011; 13:655–667. [PubMed: 21641547]
42. Sztolsztener ME, Dobrzyn A, Pikula S, Tylki-Szymanska A, Bandorowicz-Pikula J. Impaired dynamics of the late endosome/lysosome compartment in human Niemann-Pick type C skin fibroblasts carrying mutation in NPC1 gene. Mol Biosyst. 2012; 8:1197–1205. [PubMed: 22286891]
43. Elrick MJ, Yu T, Chung C, Lieberman AP. Impaired proteolysis underlies autophagic dysfunction in Niemann-Pick type C disease. Hum Mol Genet. 2012; 21:4876–4887. [PubMed: 22872701]
44. Pacheco CD, Kunkel R, Lieberman AP. Autophagy in Niemann-Pick C disease is dependent upon Beclin-1 and responsive to lipid trafficking defects. Hum Mol Genet. 2007; 16:1495–1503. [PubMed: 17468177]
45. Sorkin A, von Zastrow M. Endocytosis and signalling: intertwining molecular networks. Nat Rev Mol Cell Biol. 2009; 10:609–622. [PubMed: 19696798]

46. Kholodenko BN. Four-dimensional organization of protein kinase signaling cascades: the roles of diffusion, endocytosis and molecular motors. J Exp Biol. 2003; 206:2073–2082. [PubMed: 12756289]

47. Gschwind A, Fischer OM, Ullrich A. The discovery of receptor tyrosine kinases: targets for cancer therapy. Nat Rev Cancer. 2004; 4:361–370. [PubMed: 15122207]

48. Davies H, Bignell GR, Cox C, Stephens P, Edkins S, Clegg S, et al. Mutations of the BRAF gene in human cancer. Nature. 2002; 417:949–954. [PubMed: 12068308]

49. Stahl JM, Sharma A, Cheung M, Zimmerman M, Cheng JQ, Bosenberg MW, et al. Deregulated Akt3 activity promotes development of malignant melanoma. Cancer Res. 2004; 64:7002–7010. [PubMed: 15466193]

50. Sangai T, Akcakanat A, Chen H, Tarco E, Wu Y, Do KA, et al. Biomarkers of response to Akt inhibitor MK-2206 in breast cancer. Clin Cancer Res. 2012; 18:5816–5828. [PubMed: 22932669]

51. Zhang W, Zong CS, Hermanto U, Lopez-Bergami P, Ronai Z, Wang LH. RACK1 recruits STAT3 specifically to insulin and insulin-like growth factor 1 receptors for activation, which is important for regulating anchorage-independent growth. Mol Cell Biol. 2006; 26:413–424. [PubMed: 16382134]

52. Bromberg J, Darnell JE Jr. The role of STATs in transcriptional control and their impact on cellular function. Oncogene. 2000; 19:2468–2473. [PubMed: 10851045]

53. Frank DA. STAT signaling in the pathogenesis and treatment of cancer. Mol Med. 1999; 5:432–456. [PubMed: 10449805]

54. Niu G, Bowman T, Huang M, Shivers S, Reintgen D, Daud A, et al. Roles of activated Src and Stat3 signaling in melanoma tumor cell growth. Oncogene. 2002; 21:7001–7010. [PubMed: 12370822]

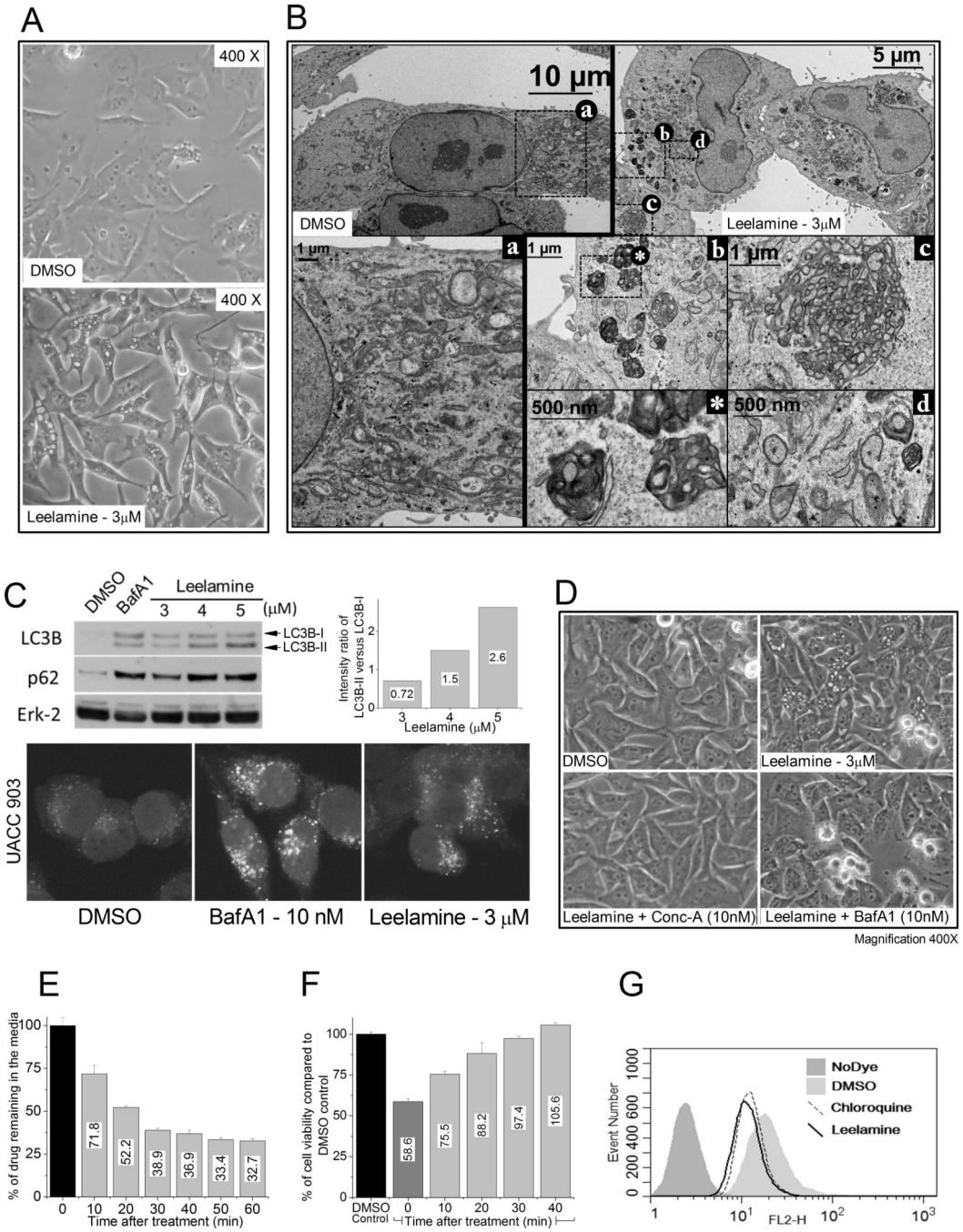

Figure 1. Lysosomotropic property of leelamine inhibits autophagic flux

A, light microscopic images show vacuolization of melanoma cells after leelamine treatment. B, transmission electron micrographs show DMSO-treated control cells (a), leelamine-treated cells displaying formation of lipofuscin-like material (b), web-like membrane whorls (c), and increased number of autophagosomes (d). C, Western blot analyses showing LC3B and P62 protein levels as a marker of autophagic flux; Erk-2 served as a loading control. BafA1 treatment was used as a positive control for inhibition of autophagic flux. Bottom, confocal microscopy of GFP-tagged LC3B accumulation in

leelamine- or BafA1-treated UACC 903 cells. D, light microscopic images of melanoma cells following leelamine treatment either alone or in combination with V-ATPase inhibitors Conc-A and BafA1. E, kinetics of 3H-labeled leelamine uptake. F, viability of cells exposed to conditioned media that is collected from leelamine-treated melanoma cells at different time points. G, histogram showing lysosomotropic property of leelamine, assessed by its competition with LysoTracker Red DND-99 dye, which was similar to chloroquine, a well-known lysosomotropic compound.

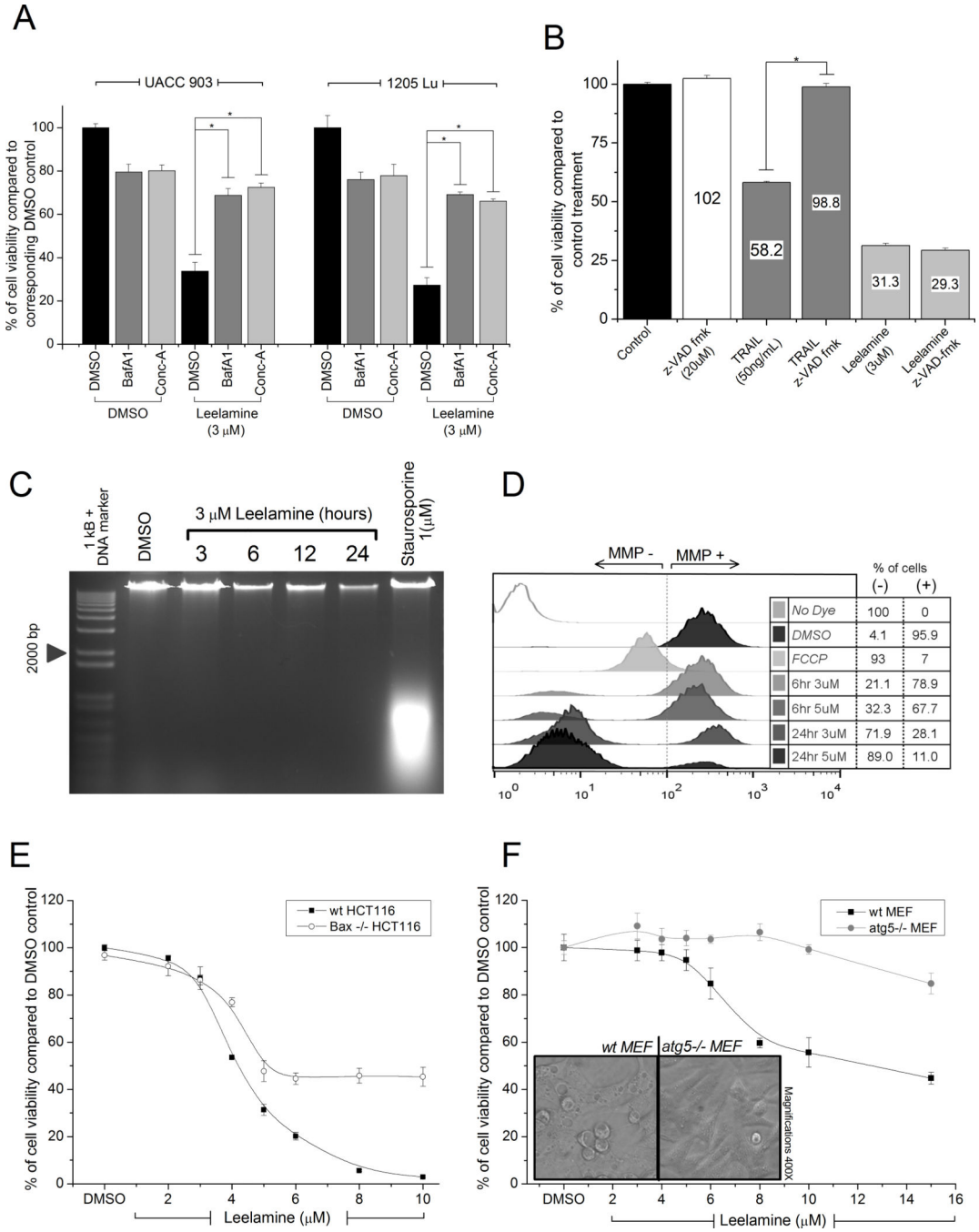

Figure 2. Lysosomotropic property of leelamine induced caspase-independent cell death leading to disruption of ΔΨm

A, viability of melanoma cells treated with leelamine in the absence or presence of V-ATPase inhibitors BafA1 or Conc-A. B, caspase dependence of leelamine-mediated cell death measured through treatment of melanoma cells with leelamine in the absence or presence of pan-caspase inhibitor, z-VAD-fmk. C, DNA laddering assay showing absence of DNA fragmentation following leelamine treatment. Staurosporine was used as a positive control for apoptosis-mediated DNA fragmentation. D, histogram showing ΔΨm following leelamine or FCCP (positive control) treatment. E, viability of wild-type or BAX-knockout

HCT116 cells after 24 hours of treatment with increasing concentrations of leelamine. F, viability of wild-type or atg5-knockout MEF cells after 24 hours of treatment with increasing concentrations of leelamine. Images showing that leelamine did not cause vacuolization of ATG5-knockout MEF cells. (*, $P < 0.05$, t test.)

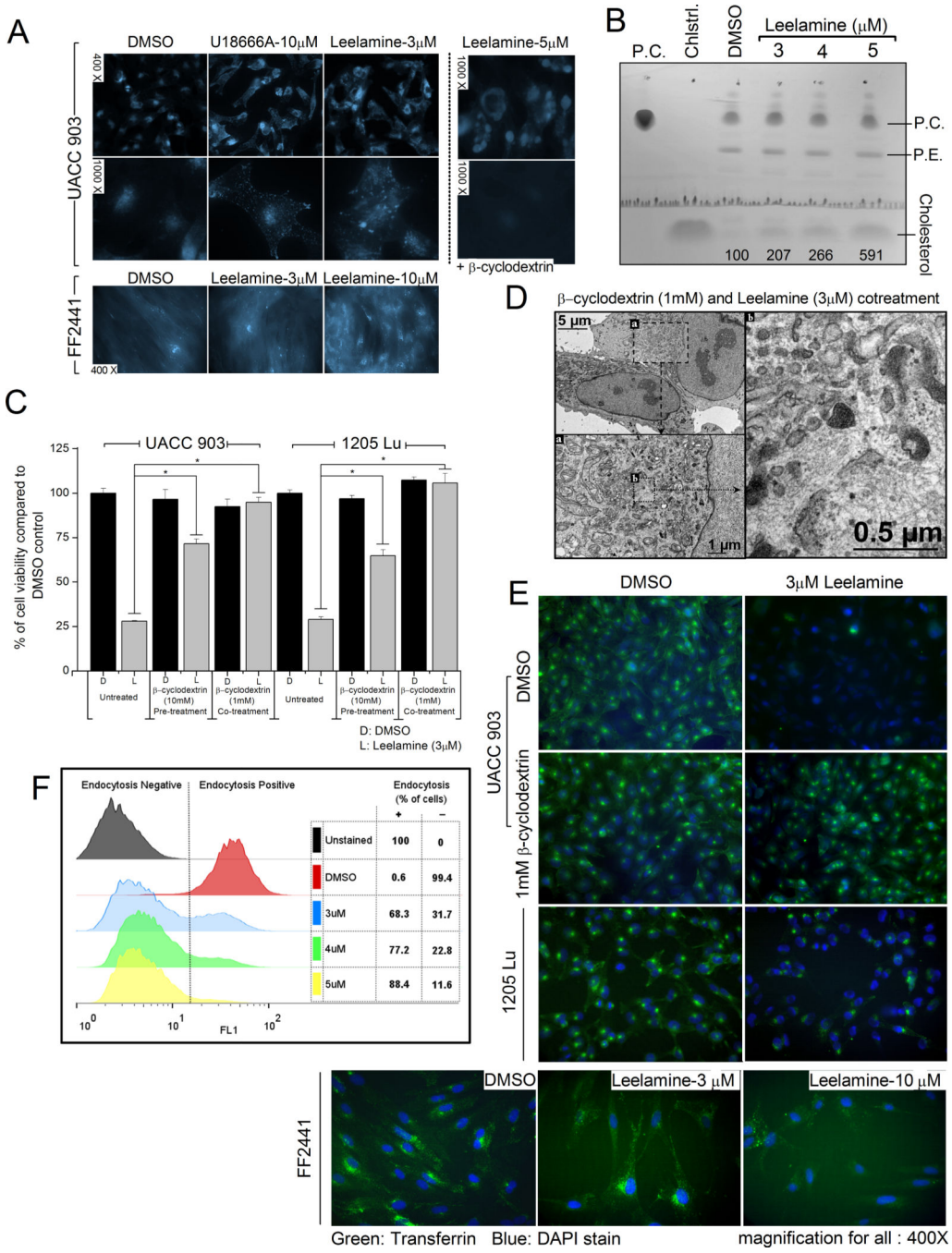

Figure 3. Leelamine-mediated cell death depends on intracellular cholesterol accumulation causing inhibition of cellular endocytosis

A, florescence microscopy of cholesterol localization following leelamine or U18666A treatment. β-cyclodextrin–mediated depletion of cholesterol prevents leelamine-mediated intracellular cholesterol accumulation (right). B, HPTLC showing cholesterol accumulation in melanoma cells with increasing leelamine concentrations. The numbers under the cholesterol band show the quantitation of the cholesterol band with respect to the DMSO treatment; PC, phosphatidylcholine; PE, phosphatidylethanolamine. C, viability of melanoma cells following leelamine treatment alone or in combination with co- or

pretreatment with β-cyclodextrin. D, transmission electron micrographs of leelamine- and β-cyclodextrin–cotreated UACC 903 cells. E, fluorescence microscopic images showing endocytosis of Alexa Fluor–conjugated transferrin protein following DMSO control or leelamine treatment in the absence or presence of β-cyclodextrine–mediated cholesterol depletion. F, flow cytometry–based analyses of Alexa Fluor–conjugated transferrin protein endocytosis following leelamine treatment. DAPI, 4′,6-diamidino-2-phenylindole. (*, $P < 0.05$, t test.)

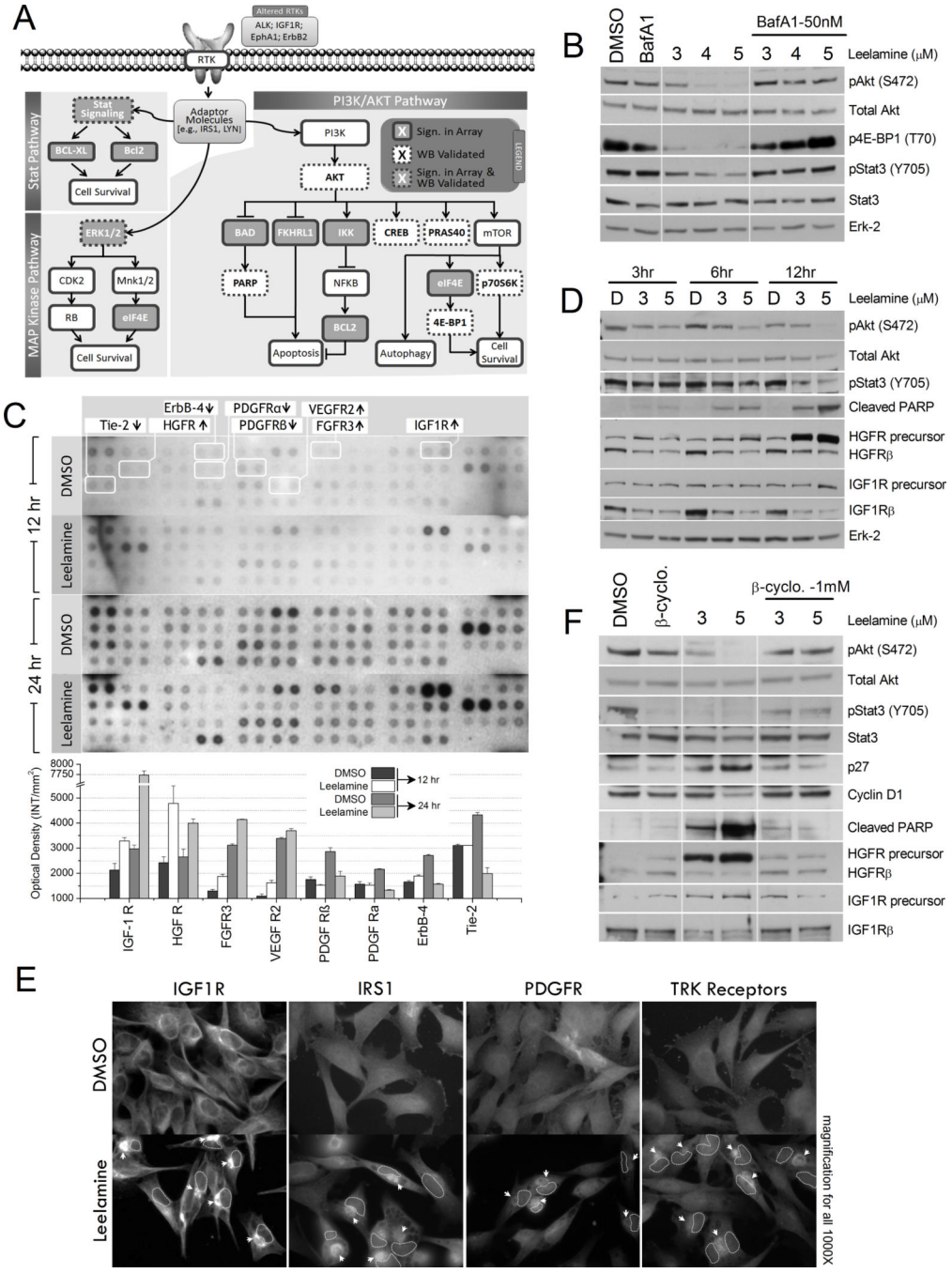

Figure 4. Leelamine mediated alterations in signaling pathways

A, schematic summary of signaling alterations in melanoma cells occurring following leelamine treatment based on Kinexus antibody array analysis. B, Western blot (WB) analysis of pAKT (S472), total AKT, 4EBP1(T70), pSTAT3(Y705), STAT3, and ERK-2 proteins in melanoma cells treated with increasing concentrations of leelamine with or without BafA1. C, RTK protein array analysis showing activity of various RTKs following leelamine treatment. D, Western blot analysis of pAKT (S472), total AKT, pSTAT3 (Y705), cleaved PARP, HGFR, IGF1R, and ERK-2 proteins post leelamine treatment of UACC 903

cells. E, immunofluorescence staining showing perinuclear accumulation (arrow heads) of RTK signaling members (nucleus marked with dashed circles in treated cells). F, Western blot analysis shows restoration of leelamine mediated signaling alterations in pAKT (S472), total AKT, pSTAT3(Y705), STAT3, CDKN1B (P27), CCND1 (Cyclin D1), cleaved PARP, HGFR, and IGF1R proteins following cholesterol depletion using β-cyclodextrine (β-cyclo) treatment. ERK, extracellular signal-regulated kinase; CDK, cyclin-dependent kinase; RB, retinoblastoma; IKK, inhibitor of IκB kinase; FGFR, fibroblast growth factor receptor.

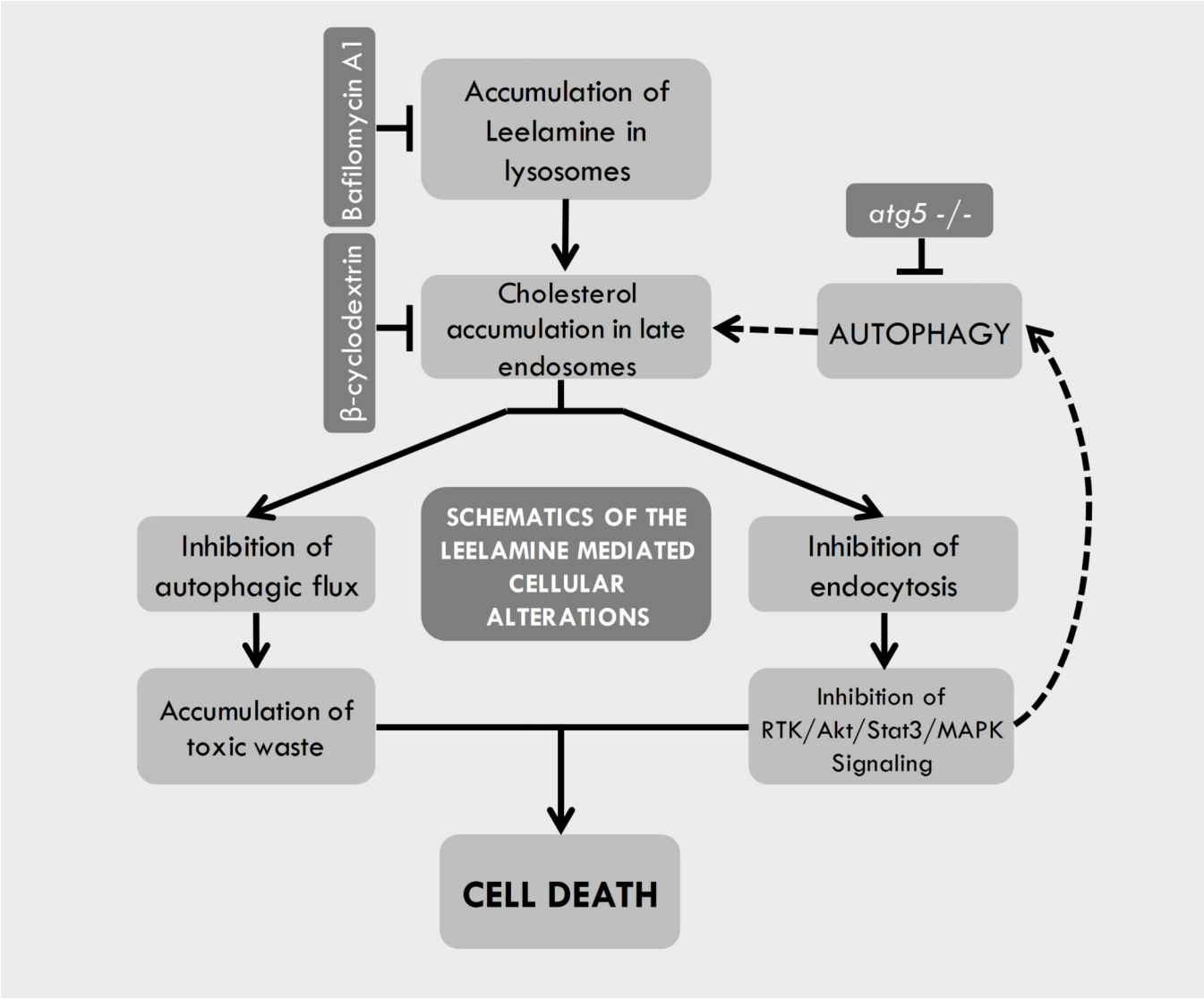

Figure 5. Schematic summary of cellular alterations mediated by leelamine in melanoma cells

Mol Cancer Ther. Author manuscript; available in PMC 2015 March 25.

Table 1

Alterations in protein expression or activity following leelamine treatment.

			Z Ratios				%CFC			
	Target Protein	**Phospho Site**	**3 hr**	**6 hr**	**12 hr**	**24 hr**	**3 hr**	**6 hr**	**12 hr**	**24 hr**
UP REGULATED	IRS1	Y1179	**1.50**	**2.95**	**2.38**	1.45	113	907	406	120
	IRS1	S312	**1.81**	**1.82**	**1.89**	**2.19**	142	307	324	288
	IR/IGF1R	Y1189/Y1190	1.21	**1.83**	**1.81**	0.17	79	328	220	8
	p38a MAPK	Pan-specific	1.35	**5.17**	**1.95**	0.70	90	2654	205	42
	PKCl/i	T564	**1.82**	0.55	0.80	**1.66**	174	84	99	163
	STAT4	Pan-specific	* **7.70**	**1.54**	**4.10**	0.31	11598	108	1162	9
	GCK	Pan-specific	* 1.39	* **2.23**	**7.44**	**1.68**	2677	5468	38746	138
	Tau	T548	**1.73**	**1.50**	* **2.14**	−0.62	141	261	298	−27
	Erk1/2	Pan-specific	0.01	**2.24**	0.89	**1.82**	−3	509	32	138
	Hsp90	Pan-specific	* **−10.83**	**4.99**	* −0.48	**1.51**	−99	75219	2736	107
DOWN REGULATED	GFAP	S8	−1.07	0.83	**−1.69**	**−2.12**	−33	168	−52	−63
	Lyn	Y508	−0.54	−0.86	**−1.56**	**−1.99**	−18	−35	−29	−61
	MAP2K4	Pan-specific	**−2.02**	**−1.54**	−1.18	−0.83	−54	−71	−41	−32
	Bad	S75	−1.27	**−2.14**	−1.44	**−1.63**	−46	−80	−63	−64
	eIF4E	S209	−0.54	**−1.69**	−1.36	**−1.74**	−24	−68	−54	−62
	ALK	Pan-specific	−1.42	**−2.64**	**−1.75**	**−1.70**	−50	−87	−69	−63
	Bcl-xS/L	Pan-specific	* **−6.5**	**−6.51**	**−3.60**	−0.34	−90	−80	−93	−22
	IkBb	Pan-specific	* **−2.33**	**−7.45**	**−2.71**	−0.06	−37	−100	−56	−7
	Bcl2	Pan-specific	**−1.52**	−0.54	**−1.93**	* −0.66	−44	−34	−53	−27
	DAXX	Pan-specific	**−1.64**	−1.34	**−2.17**	**−2.58**	−49	−64	−70	−77
	Erk1/2	Pan-specific	**−1.69**	−1.04	**−2.00**	**−1.80**	−46	−47	−50	−58
	GSK3ab	Pan-specific	**−3.11**	−1.35	**−1.88**	**−1.88**	−72	−59	−53	−62
	GSK3ab	Pan-specific	**−2.07**	−1.01	**−1.57**	−0.64	−54	−39	−43	−18
	Mos	Pan-specific	**−1.93**	* **−1.87**	**−1.60**	−1.13	−52	−81	−49	−46

			Z Ratios				%CFC			
	Target Protein	**Phospho Site**	**3 hr**	**6 hr**	**12 hr**	**24 hr**	**3 hr**	**6 hr**	**12 hr**	**24 hr**
	DFF35/45	Pan-specific	−0.88	−0.86	**−1.95**	**−2.49**	−29	−47	−53	−53
	DNAPK	Pan-specific	−0.74	−1.12	**−2.36**	**−1.97**	−25	−60	−75	−68
	EphA1	Pan-specific	−1.30	−0.76	**−1.65**	**−2.73**	−42	−42	−52	−75
	ErbB2	Pan-specific	−1.48	−0.90	**−1.98**	**−2.36**	−46	−47	−55	−67
	FKHRL1	T32	−0.99	−0.75	**−3.70**	**−1.71**	−26	−42	−64	−46

Note: Values in bold indicate Z-Ratio > 1.5 or Z-Ratio < −1.5.

Astrix (*) indicates antibody spots which were not reliable due to technical issues.

%CFC: Percentage change from control treatment